Presented at the SPIE Annual Meeting
July 30 to August 4, 2000

Position-sensitive germanium detectors for gamma-ray imaging and spectroscopy

M. Amman and P. N. Luke

Ernest Orlando Lawrence Berkeley National Laboratory
University of California, Berkeley, California 94720

ABSTRACT

Gamma-ray imaging with position-sensitive germanium detectors offers the advantages of excellent energy resolution, high detection efficiency, and potentially good spatial resolution. The development of the amorphous-semiconductor electrical contact technology for germanium detectors has simplified the production of these position-sensitive detectors and has made possible the use of unique detection schemes and detector geometries. We have fabricated prototype orthogonal-strip detectors for gamma-ray imaging studies using this contact technology. With these detectors, we demonstrate that a gamma-ray interaction event in the detector can be located in three dimensions. This more accurate determination of the interaction event position should ultimately lead to better image resolution. We have also taken advantage of the bipolar blocking nature of the amorphous-semiconductor contacts in order to investigate the use of field-shaping electrodes. The addition of such electrodes is shown to improve the spectroscopic performance of the detectors by substantially eliminating charge collection to the inter-electrode surfaces. In addition, we demonstrate that this incomplete charge collection process can also be reduced by adjusting the properties of the amorphous-semiconductor layer. In this paper, we summarize the development of these position-sensitive detectors and present the results of our studies with the detectors.

Keywords: gamma-ray imaging, gamma-ray spectroscopy, germanium detector, position sensing, orthogonal strip

1. INTRODUCTION

Gamma-ray imaging combined with high-resolution spectroscopy together form a powerful tool that is needed for many applications including those in the areas of astronomy, environmental remediation, and nuclear safeguards monitoring. Detectors based on high-purity germanium (Ge) with their excellent energy resolution and efficiency are commonly used for spectroscopy applications. However, producing position-sensitive Ge-based detectors with the fine spatial sensitivity required for many imaging applications has been a significant technical challenge. Despite this, significant progress has been made in the development of these detectors.[1-11] The amorphous-semiconductor contact technology[10-13] in particular could potentially fulfill the needs in this area. This technology has the advantages of requiring only a single contact process for the entire detector, providing automatic passivation between detector electrodes, and allowing fine electrode segmentation for accurate position measurement.

We have produced a number of orthogonal-strip detectors based on the amorphous-semiconductor contact technology. This effort was aimed to both better refine the fabrication technology and to develop techniques to improve the performance of these detectors. In planar-geometry position-sensitive Ge detectors, position detection is normally made in only the directions parallel to the detector plane and not in the depth direction. Since gamma rays will interact at random depths within the detector, this imprecise position measurement will lead to image degradation. With our detectors, we have studied the position measurement of the gamma-ray interaction events in all three dimensions rather than just two.[14,15] The depth of interaction in these detectors is obtained from the difference in the arrival time of the holes at an electrode on one side of the detector and that of the electrons at an electrode on the opposing detector surface. This separate detection of the hole collection and the electron collection is fundamental to the technique and is aided by the small-electrode charge collection properties[16-18] achieved with the strip electrodes.

The accurate measurement of the energy deposited by an interaction event in the detector is another critical requirement of these detectors. Incomplete charge collection leading to degraded spectroscopic performance can result because of the segmented contact structure. We show that for some interaction events in our detectors, charge is not completely collected within the signal measurement time because of collection to the detector surfaces between electrode segments. Consequently, we have investigated two separate approaches to overcome this problem. In the first approach an electrode (field-shaping electrode) is added between each charge-sensing electrode. By applying the appropriate bias

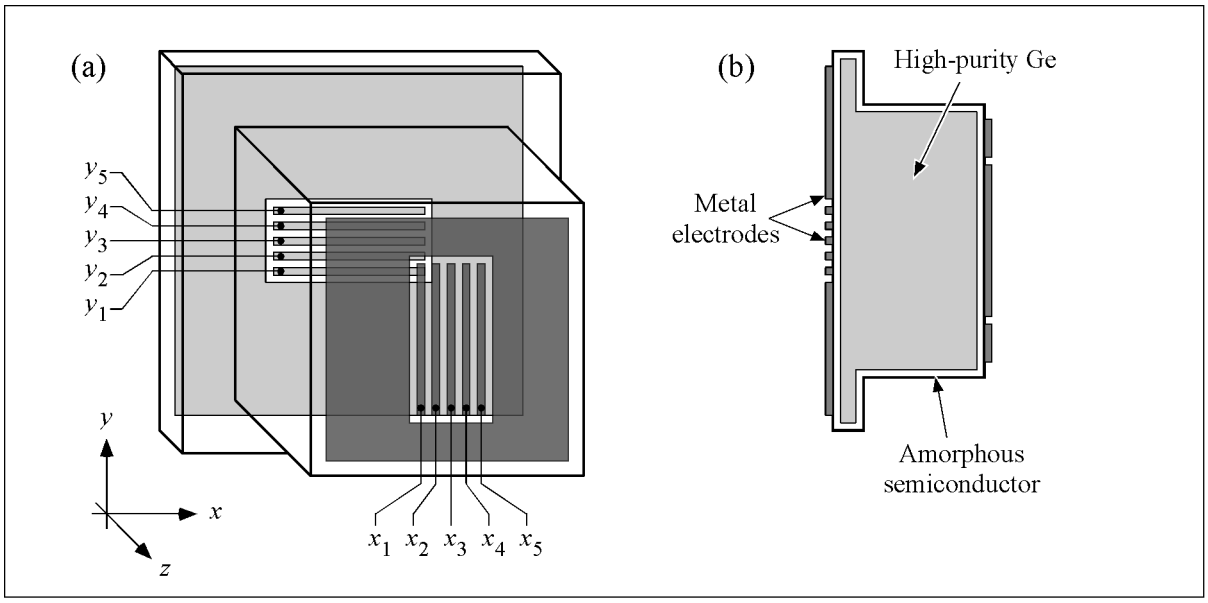

Figure 1. (a) Geometry of the prototype high-purity Ge detectors used to study the measurement of gamma-ray interaction position and energy. (b) Cross-sectional schematic diagram of the prototype detectors showing the structure of the amorphous-semiconductor contact.

between the charge-sensing electrodes and the field-shaping electrodes, efficient collection to the charge-sensing electrodes can be insured. The bipolar blocking nature of the amorphous-semiconductor contacts allows such a biasing configuration to be easily implemented. In the second approach, we adjust the resistivity of the amorphous-semiconductor layer in order to influence the charge collection to the gap surface. The idea behind this approach is that a high-resistivity surface layer might accumulate enough charge to inhibit the further collection of charge to that surface. Both of these techniques have been successful in improving the spectroscopic response of the detectors.

In this paper, we review our work on the Ge-based position-sensitive detectors. In the following section, we describe the design of the prototype orthogonal-strip detectors that we have produced for our study. Included in this description is a discussion of the structure, function, and advantages of the amorphous-semiconductor contact. Also given in this section are the details of the detector fabrication process and the measurement configuration. Following this, in Section 3, we discuss the depth sensing technique and present the results of our three-dimensional position measurements. Then in Section 4, the charge collection properties and spectroscopic performance of the detectors are presented along with the techniques developed to overcome the identified charge collection deficiency. Finally, in Section 5, we end with a summary of our work.

2. DETECTOR DESIGN, FABRICATION, AND MEASUREMENT CONFIGURATION

The typical geometry of the prototype detectors that we fabricated for this study is shown in Figure 1a. An orthogonal-strip electrode design with only a small number of strips was chosen in order to facilitate the efficient fabrication and testing of detectors during this developmental effort. The signal readout electrodes of these detectors consist of a vertical set of five strips on the front surface of the detector and an equivalent number of horizontal strips on the detector back surface. The strips have a width and spacing of 0.5 mm and are 10 mm in length. Each set of strips is surrounded by a larger than necessary guard ring in order to minimize the potential deleterious effects of surface channels[19] and excessive leakage along the side surfaces. The position-sensitive volume of these detectors is the overlap region between the two sets of strips and is approximately 5 mm × 5 mm × 10 mm for the typical detector thickness of 10 mm. The overall shape of the detectors is that of a square top hat. By design, the brim of this top hat is not depleted during detector operation. This inactive region serves as a convenient handle for use during detector fabrication and for mounting in a test fixture.

These orthogonal-strip detectors were produced using amorphous-semiconductor electrical contacts.[10-13] The basic contact structure is illustrated in the cross-sectional diagram of Figure 1b. In this structure, the contacts are formed by first coating all surfaces of the high-purity Ge crystal with a high-resistivity amorphous semiconductor (typically Ge or Si). Metal electrodes in the desired pattern are then deposited on top of the amorphous layer in order to complete the contact definition. The physical contact area in such a detector is defined by this low-resistivity metallization. However, most of the important electrical properties of the contact structure are dictated by the amorphous-semiconductor layer and the

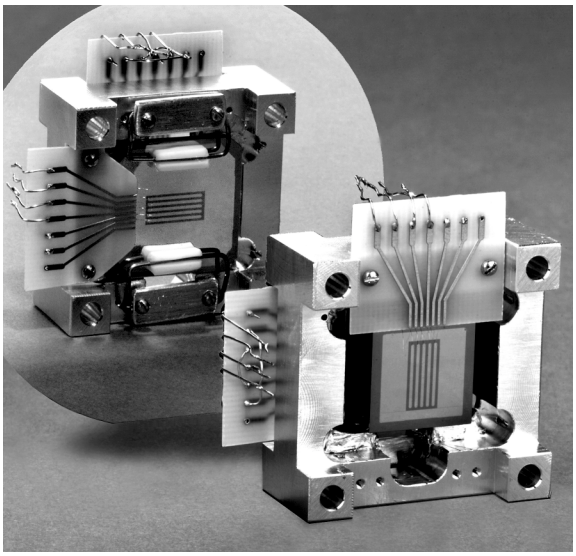

Figure 2. Photograph of a prototype orthogonal-strip Ge detector mounted in an aluminum holder.

amorphous-semiconductor to crystalline Ge interface. As a result of the disordered bonding and structural defects in amorphous semiconductors, the electronic structure of the materials is typified by energy band tailing and a substantial density of electronic states in the energy band gap.[20] The conduction at liquid nitrogen temperatures in our RF sputtered amorphous Ge (a-Ge) and amorphous Si (a-Si) films appears to be modeled best by a hopping mechanism presumably via the defect states near the Fermi energy.[21] The interface between the metal electrodes and this amorphous semiconductor is apparently ohmic in nature, whereas the amorphous-semiconductor to crystalline Ge interface behaves much like a Schottky contact. At this contact interface, the Fermi level of the a-Ge or a-Si falls near the midpoint of the crystalline Ge energy gap. This means that both electrons and holes in the amorphous semiconductor are subject to a barrier of about half the Ge band gap for injection into the crystalline Ge. Consequently, the amorphous-semiconductor contact can block the injection of both types of charge carriers. The same contact can therefore operate with low leakage current under either bias polarity. This is in contrast to conventional doped contacts which block injection under only one bias polarity, and metal to Ge surface barrier contacts that typically block well only when negatively biased.[22,23] As will be demonstrated later in this paper, this bipolar blocking nature of the amorphous-semiconductor contact enables the simple implementation of inter-strip biasing schemes.

Another important aspect of the a-Ge and a-Si films is that the defect density and, consequently, the conductivity, can be controlled by incorporating hydrogen into the films.[20] Hydrogen incorporation into our RF sputtered films is accomplished by adding hydrogen to the sputtering gas. The addition of the hydrogen can produce orders of magnitude increases in the amorphous film resistivity. This allows us to adjust the resistivity such that we achieve low inter-strip leakage while still maintaining efficient charge collection through the film.

The use of the amorphous-semiconductor contact provides several other advantages over conventional contact technologies. First, the contact is thin in contrast to the commonly used lithium-diffused contact. Second, the amorphous film acts as a passivant of the Ge crystal surface.[24] Therefore, the contact formation process automatically leads to a passivated detector. Third, a single contact technology can be used for the entire detector, thereby simplifying detector fabrication. Finally, since the physical contact electrodes are defined by the metallization, finely spaced contacts can be made simply by patterning the metallization through standard processing methods. Because of these advantages, the amorphous-semiconductor contact technology is a logical choice for the production of position-sensitive Ge detectors.

The details of the process to produce the prototype orthogonal-strip detectors are as follows. The fabrication process begins by cutting a crystal of high-purity Ge into the top hat shape with a diamond saw. The front and back detector surfaces are then lapped in order to remove the blade marks created during the cutting process. The surface damage introduced by these mechanical processes is then removed by etching the crystal in a 4:1 nitric to hydrofluoric acid mixture. Following this, the crystal is briefly etched again in fresh 4:1 etchant, quenched in methanol, and blown dry with nitrogen in order to prepare the surfaces for contact deposition. The crystal is then immediately loaded into an RF sputtering system. Amorphous-Ge or a-Si is deposited on all detector surfaces to a thickness between 50 and 100 nm. The sputtering is performed in pure argon or an argon-hydrogen mixture at a pressure of 7 mtorr. After this, metal layers forming the strip electrodes and guard rings are deposited on top of the amorphous-semiconductor layer using thermal evaporation through

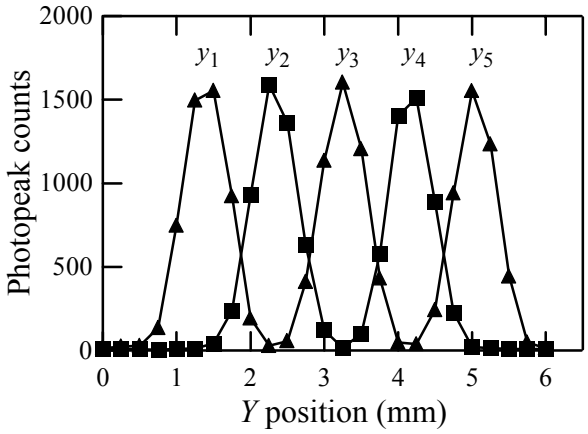

Figure 3. Integrated counts within the photopeak as a function of the collimated ^{241}Am gamma-ray source location measured with an orthogonal-strip detector of the type schematically shown in Figure 1. The source with a beam diameter of about 0.5 mm was scanned in the *y* direction along the front of the detector while the pulse-height information was acquired from the *y* strip electrodes on the back surface of the detector. Alternate *y* electrodes were interconnected for this measurement so that only two readout channels would be necessary. The detector, which fully depleted at 800 V, was operated with 1000 V applied to the front electrodes. The energy window for the integration was from 56.5 keV to 62.5 keV.

shadow masks. The metallization consists of a chromium layer about 25 nm thick to act as an adhesion layer followed by multiple gold evaporations in order to achieve a final electrode thickness of about 500 nm. This metallization scheme was found to produce good results with the wire bonding process used later to make electrical connection to these electrodes. After metallization, the detector is placed into an aluminum frame designed so that only the inactive brim of the detector contacts the frame. Finally, electrical connection to the detector electrodes is made through ultrasonic wire bonding between the electrodes and bonding pads on two circuit boards attached to the mounting frame. A photograph of a completed and mounted detector is shown in Figure 2.

Measurements were made with the orthogonal-strip detectors cooled to about 80 K inside a general-purpose test cryostat. The test configuration varied somewhat between the different measurements; however, a bias of 1000 V was typically applied to the front guard ring and strips while the back guard ring and strips were maintained at ground potential. The depletion voltage of the detectors varied between 300 V and 800 V depending on the particular detector. Ac-coupled charge-sensitive preamplifiers with cooled FET input stages were used to measure the induced charge signals from the strip electrodes. Depending on the information required, these signals were either passed through a standard pulse-processing chain for conventional pulse-height spectral measurements, or they were acquired with a digital oscilloscope and transferred to a computer for real-time analysis with LabVIEW programs. For many of the measurements, strip electrodes were interconnected in order to minimize the number of required channels of electronics readout.

3. POSITION SENSING

The location of each gamma-ray interaction event in the position-sensitive volume of our orthogonal-strip detectors can in principle be determined in three dimensions.[14,15] The position detection in the lateral dimensions of *x* and *y* is accomplished using the conventional method for orthogonal-strip electrode geometries. To see how this is done, consider a gamma-ray interaction event taking place near the center of the detector. This event will generate an equal number of free electrons and holes at the interaction site. For a positive bias applied to the front electrodes, the resultant detector field will cause the electrons to drift to the front electrodes and the holes to the back electrodes. The position of the front strip electrode that ultimately collects the electrons indicates the *x* location of the interaction event while the position of the back strip electrode that collects the holes provides the *y* location. An illustration of this position detection with one of our detectors is shown in Figure 3. Here we show the results from scanning a collimated ^{241}Am gamma-ray source (59.5 keV) along the middle *x* electrode of the front surface while measuring the charge collection events with the *y* electrodes on the back surface of the detector. For this measurement, alternate *y* electrodes were connected together (in order to minimize the number of readout channels required for the test), and pulse-height spectra were accumulated from the resulting two sets of *y* strip electrodes. Plotted in Figure 3 is the number of counts within the photopeak of the spectra acquired from these interconnected *y* electrodes as a function of the source location. As the source is scanned and the resultant hole collection

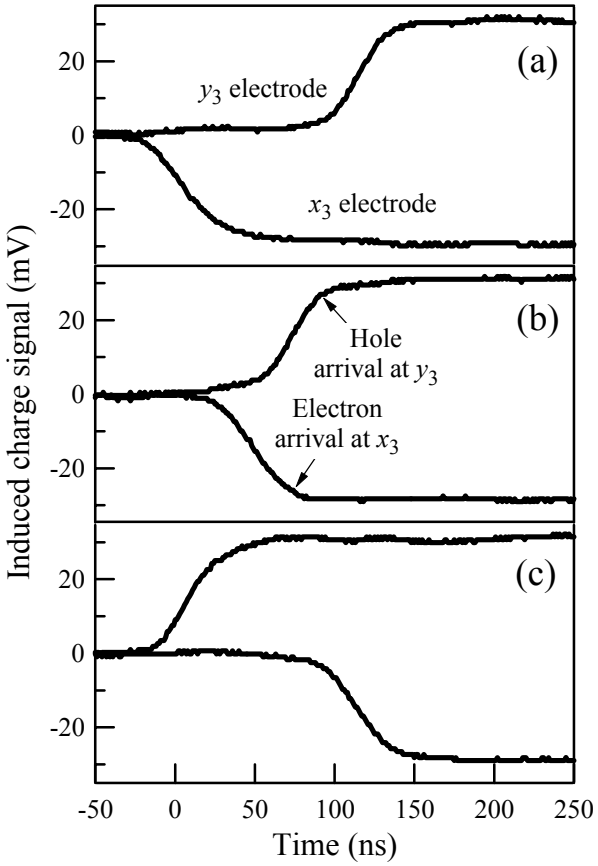

Figure 4. Measured induced charge signals from the x_3 electrode and the y_3 electrode of an orthogonal-strip detector of the type schematically shown in Figure 1. Each pulse pair shown results from the collection of the charge generated in the detector by a gamma ray from a ^{57}Co source. The detector, which fully depleted at 300 V, was operated with 1000 V applied to the front electrodes. The time difference between the occurrence of the x_3 pulse and the y_3 pulse can be used as a measure of the gamma-ray interaction depth.

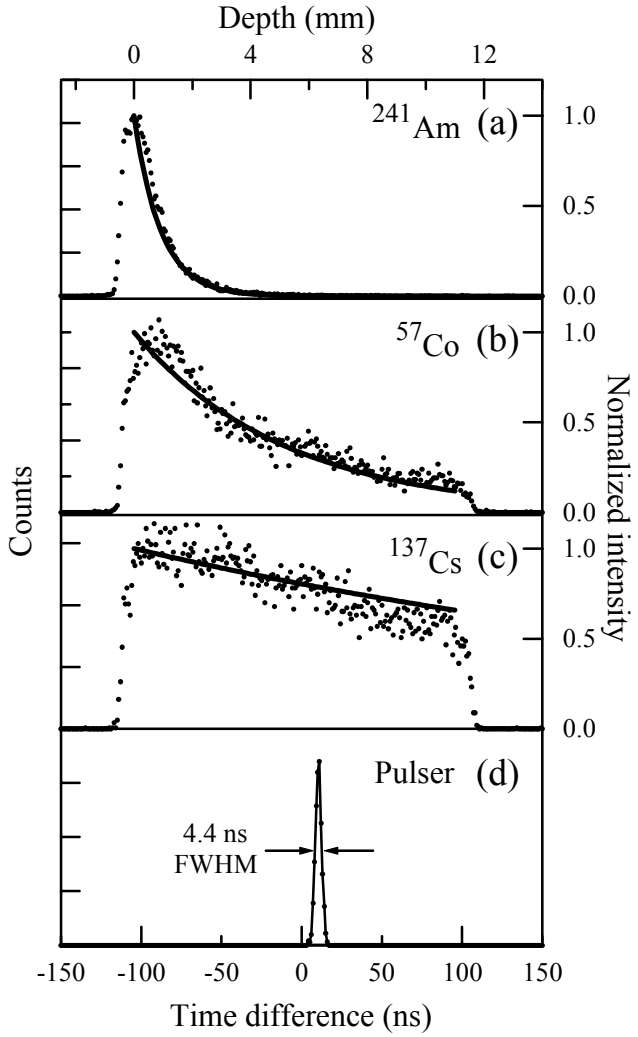

Figure 5. Time spectra acquired with an orthogonal-strip detector. Each spectrum was produced by repeatedly acquiring a coincidence pulse pair from electrodes x_3 and y_3, measuring the time difference between the x_3 electrode pulse and the y_3 electrode pulse, and then incrementing the channel number in the spectrum corresponding to the measured time difference. The location of each pulse was taken to be the time at which the pulse reached its half-maximum magnitude value. A separate time spectrum (dots) was measured for each of the following sources placed in front of the detector: (a) ^{241}Am, (b) ^{57}Co, and (c) ^{137}Cs. The detector bias used for these measurements was 1000 V. For comparison, the expected exponential decay in the intensity of the gamma rays with depth (solid lines) is superimposed on top of the measured spectra. A time spectrum acquired when periodic electronic pulse signals were simultaneously applied to the x_3 and y_3 electrodes is plotted in (d). The pulse height used corresponds to a 59.5 keV gamma-ray event. The width of the peak in this spectrum is a measure of the uncertainty in the depth determination introduced by the noise of the measurement electronics.

moves from one y strip electrode to the next, the photopeak counts from each of the two electrode sets is observed to rise or fall as expected, thereby demonstrating good y position sensitivity. Likewise, the front strip electrodes behave similarly for the measurement of the event location in the x direction.

The measurement of only the lateral location of each gamma-ray interaction, as is conventionally done, can lead to a loss of image resolution. The deeply penetrating nature of energetic gamma rays enables the imaging of sources through intervening matter. However, from the detection standpoint, this nature of the gamma rays presents a problem. Relatively thick detectors are required in order to stop these gamma rays. The random nature of the gamma-ray interaction leads to a random depth of interaction (z location) within the detector. Since the interaction events do not necessarily occur at the same depth, parallax image broadening will result. This loss of image resolution can be mitigated, however, through the measurement of the depth of interaction for each event. Such a measurement can be made based on the time difference in the electron arrival at the anode and the hole arrival at the cathode. For example, if the electron arrival occurs much sooner than the hole arrival, the interaction must have taken place near the anode, whereas if the opposite is true, the event must have occurred near the cathode. The extraction of these arrival times with an orthogonal-strip electrode geometry is facilitated by the small electrode effect.[16-18] Consider again the situation of a gamma-ray interaction event taking place near the center of the positive-biased detector. Under the influence of the applied bias, the generated carriers drift and separate. In contrast to a simple planar detector with full-area electrodes, little charge is initially induced on the particular x and y strip electrodes that will eventually collect the electrons and holes (referred to as electron-collecting electrode and hole-collecting electrode, respectively). This is because the nearby electrode strips and guard ring on both sides of the detector act to partially screen the collecting electrodes from the drifting carriers. This changes when the drifting charge moves into close vicinity of a collecting electrode. At this point, there is a rapid rise in the induced charge on that particular electrode which continues until the drifting charge is fully collected on the electrode. This type of charge induction is the basis of the small electrode effect. The rapid rise in the induced charge signal on the electron-collecting electrode marks the arrival of the electrons at that electrode, and likewise the rapid signal rise on the hole-collecting electrode marks the arrival of the holes. The essential element here is that the collection of the electrons and the collection of the holes are each separately detected. The difference in the arrival times for these two signals can then be easily extracted and used to determine the depth of the gamma-ray interaction.

We have experimentally investigated this depth of interaction sensing method using our prototype orthogonal-strip detectors. A set of induced charge signals obtained from one of the detectors is shown in Figure 4. The signals are those from the x_3 and y_3 electrodes. Each pulse pair shown results from the collection to these electrodes of the charge generated by a gamma ray from a ^{57}Co source (122 keV) placed facing the front surface of the detector. For the event of Figure 4a, the electron arrival at x_3 precedes the hole arrival at y_3 by about 100 ns. This is roughly the time required for holes to drift from one side of the detector to the other. Therefore, the gamma ray that gave rise to these signals must have interacted very near the front detector surface. In contrast to this are the pulses of Figure 4c in which the y_3 pulse precedes the x_3 pulse by about 100 ns. This is indicative of an interaction event near the back detector surface. Finally, the near simultaneous pulses of Figure 4b are consistent with an event near the center of the detector.

To confirm experimentally that the time separation between each corresponding x_3 pulse and y_3 pulse relates to the gamma-ray interaction depth, we have acquired time spectra with the detector when separately exposed to ^{241}Am, ^{57}Co, and ^{137}Cs (661.7 keV) gamma-ray sources. The spectra were each obtained by repeatedly doing the following: acquiring a pulse pair, measuring the time difference between the occurrence of the x_3 pulse-height half-maximum and the occurrence of the y_3 pulse-height half-maximum, and incrementing the count in the channel number corresponding to the measured time difference. The pulse pairs were acquired using a digital oscilloscope, transferred to a PC, and then analyzed in real time using programs written in LabVIEW. The threshold for triggering an acquisition event during this process was set to about 15 keV for both electrode signals. Spectra gathered using this technique are shown in Figure 5. The bottom axis of these plots represents the y_3 pulse location in time subtracted from the x_3 pulse location. Therefore, negative time differences of about -100 ns correspond to gamma rays that interacted near the x_3 electrode, whereas time differences of about 100 ns resulted from events near the y_3 electrode. The measured time distributions clearly depend on the energy of the incident gamma rays. As expected, the lower energy gamma rays predominantly produced events near the entrance (front) side of the detector (Figure 5a), whereas the higher energy gamma rays led to a more uniform distribution of the events with depth (Figure 5c). Each of these distributions can be compared to the simple exponential attenuation of the gamma-ray intensity with depth. Using attenuation coefficients appropriate for the specific gamma-ray energies,[25] we have calculated the expected distributions and superimposed them onto the spectra of Figure 5. For simplicity, we have assumed here a linear relation between the depth of interaction and the measured time difference. The measured and calculated distributions are in good agreement with each other, thus confirming the accuracy of this technique. The depth position resolution achieved with this technique will in part be limited by the electronic noise of the electrode signals. To quantify this contribution to the position resolution broadening, we simultaneously applied a periodic electronic pulse signal to both the x_3 electrode and the y_3 electrode and then accumulated a time spectrum. A pulse height corresponding to that of a

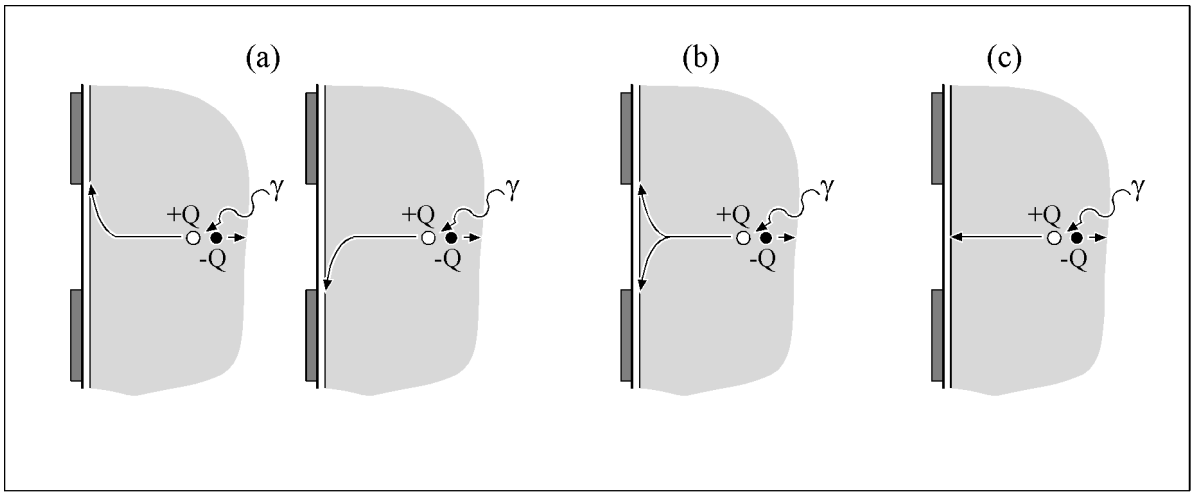

Figure 6. Schematic diagrams illustrating the types of charge collection that can take place for a gamma-ray interaction event that occurs between two electrodes. The charge can be (a) completely collected by either electrode, (b) shared between the two electrodes, or (c) collected to the surface between the two electrodes.

59.5 keV gamma-ray event was used. The resulting spectrum shown in Figure 5d has a peak with a width of 4.4 ns. This corresponds to a depth position resolution of about 0.25 mm and illustrates that in principle highly accurate depth sensing can be achieved even for relatively low energy events.

4. CHARGE COLLECTION AND SPECTROSCOPY

The position sensitivity of our detectors relies on finely dividing into a number of strips the normally full-area anode and cathode of a conventional planar detector. This act of segmenting the electrodes can lead to degraded detector performance. One of the primary physical causes of the degraded performance is the existence of weak lateral electric field regions between adjacent strip electrode segments. As an illustrative example, consider the case of a gamma ray interacting between electrodes y_2 and y_3 of the detector in Figure 1. The electric field set up in the detector by a positive bias applied to the front electrodes causes the generated holes to drift towards the y_2 and y_3 electrodes. However, since both electrodes are at the same potential, it is not clear what will happen to the holes when they drift near the two strips. A number of possibilities are illustrated in Figure 6. If the potential of the detector surface between the two electrodes is sufficiently more positive than the electrodes, the charge could potentially be efficiently collected to the electrodes. For such a situation the holes could be collected to either y_2 or y_3 (Figure 6a) or shared between the two electrodes (Figure 6b). The energy deposited by the gamma ray is accurately determined for the cases in which the charge is fully collected to either of the electrodes. Additionally, for the case when the charge is shared between the electrodes, the full energy signal can be recovered by summing together the two individual electrode signals.[26] Consequently, no significant loss of detector performance is expected under these circumstances. Another possibility, though, is that little or no lateral (y direction) electric field exists to cause the holes to be completely collected by the electrodes within the pulse measurement time. In this case the holes would be collected to the detector surface between the two electrodes and then would slowly drift the remaining distance to the electrodes (Figure 6c). Since the holes may not be completely collected to the electrodes within the pulse measurement time, even the summed signal will have a deficit. A loss of either or both energy resolution and photopeak efficiency will result.

To determine which of these situations exists in our detectors, we have analyzed the detector response to events occurring between electrodes. This was accomplished by probing the front of the detectors with a finely collimated ^{241}Am gamma-ray source while acquiring induced charge signal data from the backside y electrodes. The gamma-ray source used produced a beam about 0.5 mm in diameter and was mounted on an x-y translation stage so that the detector response could be measured as a function of the gamma-ray interaction location. To reduce the number of readout channels required for this measurement, alternate y electrodes were connected together. The interconnected electrodes y_2 and y_4 will be referred to as even electrodes and the electrodes y_1, y_3, and y_5 as odd electrodes. The source was then positioned between electrodes y_2 and y_3. At this location, the pulse height measured at the even-electrode readout channel is mainly a result of the charge induction on the y_2 electrode while the pulse height measured at the odd-electrode readout channel results primarily from

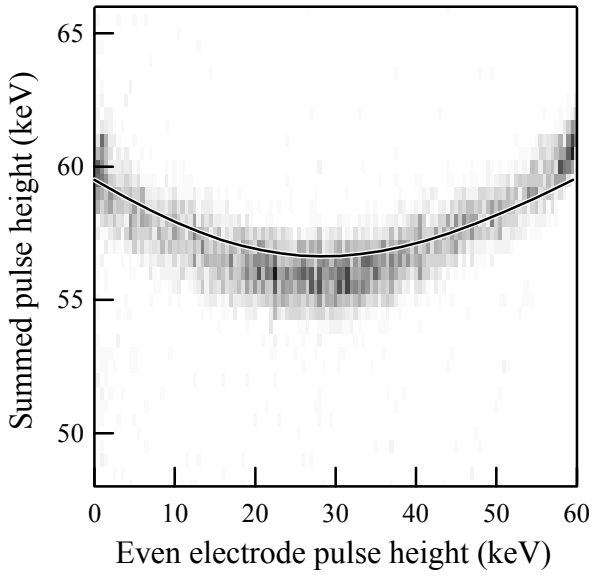

Figure 7. Intensity plot of measured gamma-ray interaction events that occurred in the gap between electrodes y_2 and y_3 of an orthogonal-strip detector. This data was acquired by positioning a collimated ^{241}Am gamma-ray source in front of the detector and measuring the induced charge pulses from the y electrodes interconnected into even (y_2 and y_4) and odd (y_1, y_3, and y_5) electrode sets. The detector, which fully depleted at 300 V, was operated with 1000 V applied to the front electrodes. For each event, the summed energy from the even and odd electrodes is plotted against the energy from the even electrodes. The darkness of each pixel in the plot is indicative of the number of events that fell within the energy window of the pixel. A darker pixel contains more events than does a lighter one. The dip in the distribution indicates a pulse-height deficit for events occurring in the gap between y_2 and y_3. For comparison, the calculated total pulse height as a function of the pulse height from the even electrodes is plotted (solid line). These pulse heights were determined by assuming that the generated holes were collected directly to the detector surface between electrodes y_2 and y_3 and not completely to either electrode.

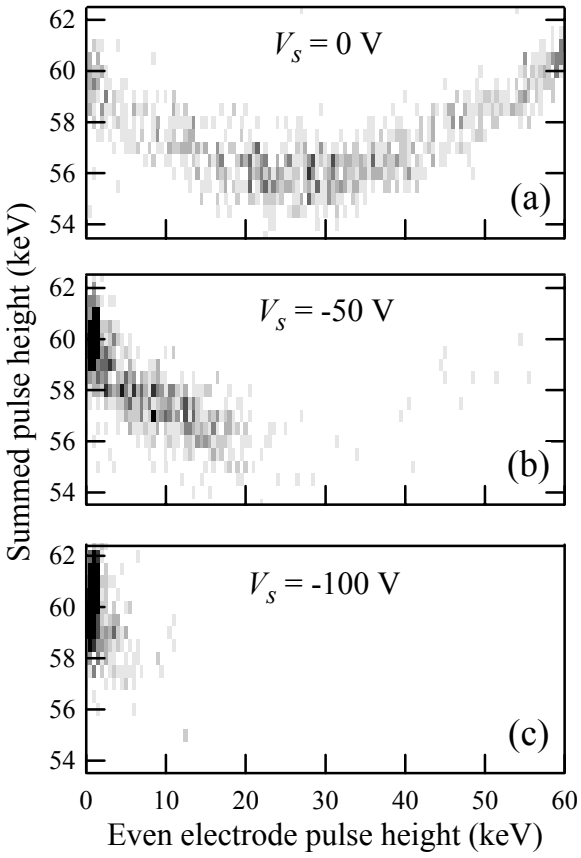

Figure 8. Intensity plots of measured gamma-ray interaction events that occurred in the gap between electrodes y_2 and y_3 of an orthogonal-strip detector. This data was acquired in the same manner as that of Figure 7 except that in this case a sensing-electrode bias V_s was applied to the odd electrodes. The values of this bias used to obtain the plots were (a) 0 V, (b) -50 V, and (c) -100 V. This sensing-electrode bias can substantially eliminate the dip in the intensity plot distribution by forcing a more complete collection of the charge to the odd electrodes (sensing electrodes).

the charge induction on the y_3 electrode. This pulse-height information was then accumulated for events that produced a pulse on either or both of the two readout channels. An instructive representation of such data acquired with one of our detectors is shown in the intensity plot of Figure 7. Here the summed pulse height (of the even and odd electrodes) for each acquired event is plotted against the even-electrode pulse height for that event. Each gray pixel in the plot represents an energy window into which at least one interaction event fell. The darkness of a pixel is representative of the number of events that are contained within the energy window of that pixel. A greater number of events result in a darker pixel. For a charge collection situation of the type shown in Figure 6a, an intensity plot of this type would contain a high intensity distribution (dark spot) at a summed pulse height of 59.5 keV in combination with an even-electrode pulse height of zero (complete collection to y_3) or 59.5 keV (complete collection to y_2). For the ideal charge-sharing situation of Figure 6b, the summed pulse height would always correspond to the gamma-ray energy of 59.5 keV while the even-electrode pulse height could vary between zero and 59.5 keV. Neither of these situations, however, accurately describes the data of Figure 7. From this figure, we see that when the induced charge signal is shared between the two sets of electrodes, a pulse-height deficit is observed in the summed signal. This deficit is a maximum when the two sets of electrodes equally share the signal presumably as a result of an event occurring midway between the y_2 and y_3 electrodes.

Using a simple model of the detector, we can determine if the measurements of Figure 7 are consistent with the idea of charge collection to the surface between the two electrodes as illustrated in Figure 6c. In this model, the electrons

generated by each gamma-ray interaction event are assumed to be fully collected by the front x_3 electrode and the holes fully collected to the surface between the y_2 electrode and the y_3 electrode. The electron and hole charge clouds are also assumed to be point-like in this calculation. We are therefore neglecting the effects caused by the finite size of the initially generated charge clouds and the subsequent spreading by diffusion.[27] With these assumptions, we have calculated the total induced charge pulse height from the even and odd electrodes as a function of the pulse height from the even electrodes alone using the weighting potential method.[28,29] The result of the calculation is the solid line plotted in Figure 7. The calculated response matches reasonably well with the measured data and predicts a maximum charge collection deficit of about 5 %. This deficit is a direct consequence of the incomplete collection of the holes to the y electrodes. Based on the above measurements and this modeling result, it is apparent that incomplete charge collection resulting from a weak lateral electric field between electrodes is present in this detector. Left uncorrected this will lead to degraded detector performance.

One method to overcome this problem is to introduce a potential difference between adjacent electrodes. This can be accomplished by using only every other electrode for signal readout. These charge-sensing electrodes would each be connected to a separate readout channel. The remaining strip electrodes would then be interconnected to act as field-shaping electrodes. Through the application of an appropriate bias between the field electrodes and the sensing electrodes, the weak lateral electric field at the detector surface can be eliminated, thereby enabling complete charge collection to the sensing electrodes. Such a detection scheme would be difficult to implement, though, with the conventional boron-implanted (p^+) or lithium-diffused (n^+) contact technologies used with Ge detectors. These contacts are either non-injecting for electrons or for holes, but not for both. Consequently, the application of the necessary bias between two adjacent boron-implanted strips, for example, would lead to a substantial leakage current as a result of hole injection at the positively biased strip. Alternate p^+ and n^+ contacts would have to be produced to avoid this problem. A considerable advantage of the amorphous-semiconductor contacts is that they do not suffer from this limitation. These contacts can exhibit good blocking behavior under either bias polarity and thereby allow the direct implementation of the field-shaping detection scheme. To determine the effectiveness of using field-shaping electrodes, the detector used to acquire the data of Figure 7 was connected and tested as previously described except with the addition of a negative bias V_s applied to the odd electrodes. We are therefore using the interconnected even electrodes as field-shaping electrodes, while the odd electrodes are the sensing electrodes. The results of measurements at three different sensing-electrode biases are shown in Figure 8. This figure shows that with the addition of V_s, the dip in the distribution of the events, which indicates a pulse-height deficit (Figure 8a), can be largely eliminated by forcing complete collection at the sensing electrodes (Figure 8c). This then improves the detector performance as the spectroscopic measurements of Figures 9 and 10 demonstrate. Each spectrum in these figures was acquired by placing a gamma-ray source facing the front side of the detector and measuring the signals from the individual sensing electrode y_3. The measurements in part (a) of these two figures were made with the sensing electrodes at the same ground potential as the field electrodes. The measurements in part (b) of the figures were then made with a sensing-electrode bias of -200 V. In comparing the ^{241}Am spectra of Figures 9a and 9b, we see that the application of the sensing-electrode bias substantially increased the counts in the photopeak by allowing the charge from events within the inter-electrode regions and beneath the nearby field electrodes to be fully collected. The background counts were also reduced as a result of a decrease in the number of events with incomplete charge collection. Additionally, the application of the sensing-electrode bias did not measurably increase the electronic noise as the pulser widths indicate, and the energy resolution at 59.5 keV improved slightly. The ^{137}Cs spectra of Figures 10a and 10b further demonstrate the performance improvements achieved with this technique. Of particular significance is the reduction of low-energy background counts.

It is clear that the field-shaping scheme can improve the performance of a detector by avoiding charge collection to the inter-electrode surface. However, the technique does have drawbacks. First, it requires additional biases and as a result can necessitate ac coupling of all the readout channels. Second, an additional set of field-shaping electrodes is needed. An alternative approach to improve the detector performance without these added complications is to reduce the gap between electrodes. By reducing this gap, the charge collected to the gap surface ends up closer to the surrounding electrodes, thereby producing a smaller pulse-height deficit. This approach also has its drawbacks though. By decreasing the spacing between strips, the inter-strip capacitance will increase, which will lead to an increase in the detector noise. Furthermore, the finer electrode spacing may require a more complex electrode fabrication technique such as photolithography.

We have investigated a third approach to improve the charge collection in our orthogonal-strip detectors. The basic idea behind this approach is to inhibit the charge collection to the inter-electrode surface by modifying the properties of the amorphous-semiconductor film on this surface. Specifically, if the film is high enough in resistivity, a sufficient amount of charge could be collected to and accumulated within the film to prevent subsequent charge collection to the surface. To test this idea, we reprocessed the detector used to obtain the data of Figures 7 and 8. This detector was originally fabricated with an a-Ge contact layer that was sputtered in pure argon. The resistance between strips on this detector was measured to be about 9×10^{11} Ω. After the measurements with this detector were completed, the detector was reprocessed as before

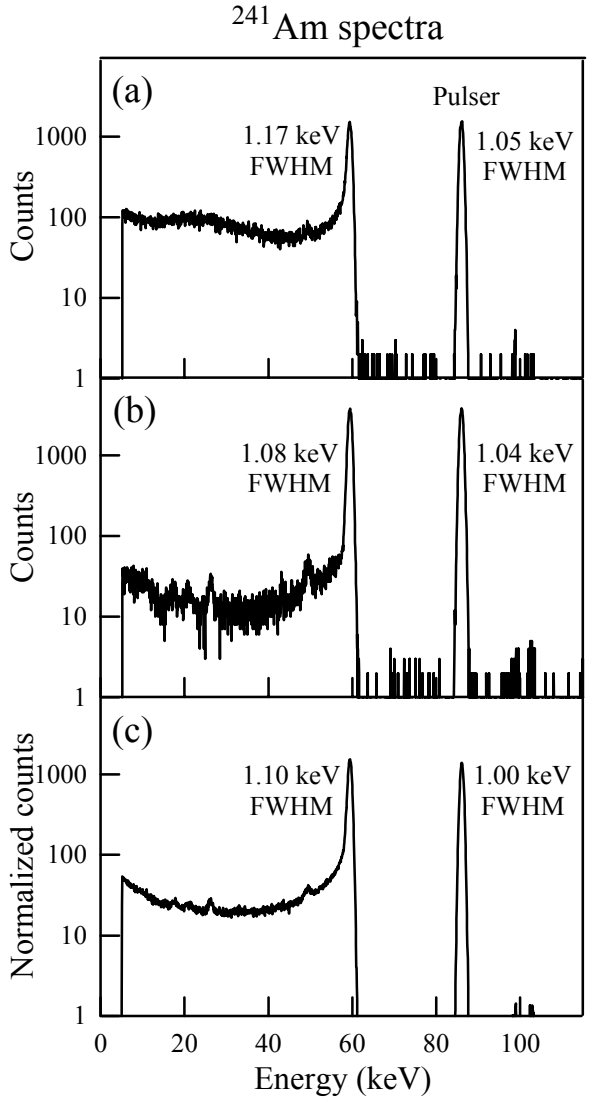

Figure 9. ^{241}Am pulse-height spectra acquired from the y_3 electrode of an orthogonal-strip detector. The source was placed facing the front of the detector for this measurement, and the detector was operated at a bias of 1000 V. For the spectra of (a) and (b), the electrodes y_2 and y_4 were interconnected and used as field electrodes by connecting them to ground potential. The sensing electrodes y_1, y_3, and y_5 were all held at the potential V_s and isolated from each other so that signals could be measured from each one separately. A spectrum was measured without the addition of field shaping, (a) V_s = 0 V, and with the added benefit of field shaping, (b) V_s = -200 V. The spectrum of (c) was acquired with this same detector after it was reprocessed with a higher resistivity amorphous-semiconductor contact layer. For this case, field shaping was not used.

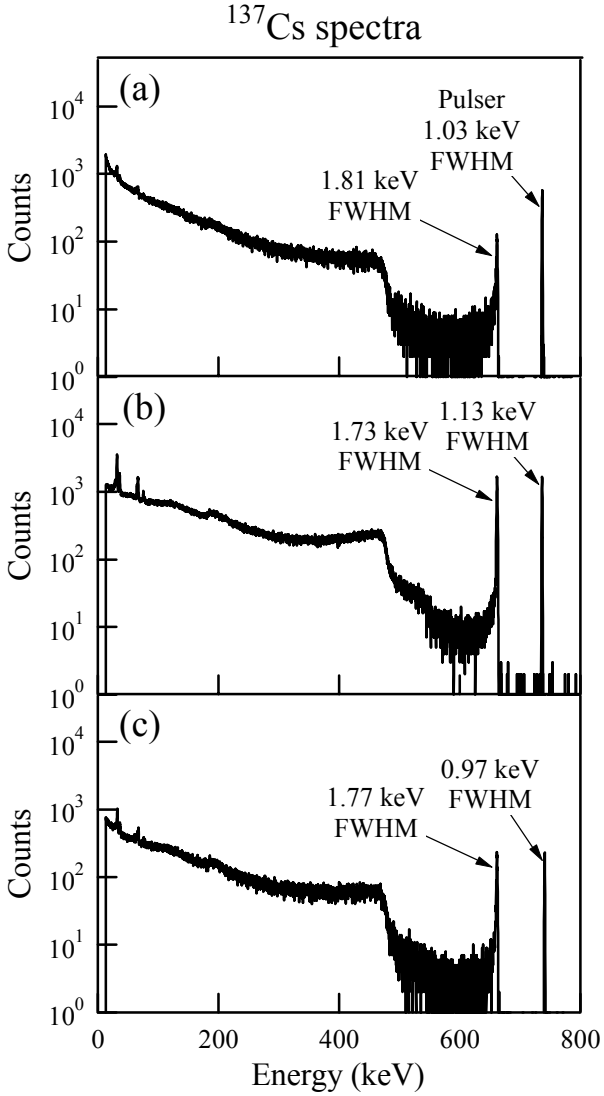

Figure 10. ^{137}Cs pulse-height spectra acquired from the y_3 electrode of an orthogonal-strip detector. The source was placed facing the front of the detector for this measurement, and the detector was operated at a bias of 1000 V. For the spectra of (a) and (b), the electrodes y_2 and y_4 were interconnected and used as field electrodes by connecting them to ground potential. The sensing electrodes y_1, y_3, and y_5 were all held at the potential V_s and isolated from each other so that signals could be measured from each one separately. A spectrum was measured without the addition of field shaping, (a) V_s = 0 V, and with the added benefit of field shaping, (b) V_s = -200 V. The spectrum of (c) was acquired with this same detector after it was reprocessed with a higher resistivity amorphous-semiconductor contact layer. For this case, field shaping was not used.

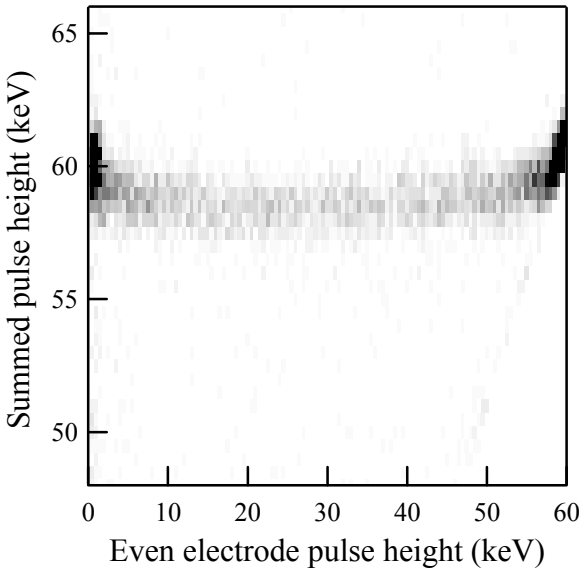

Figure 11. Intensity plot of measured gamma-ray interaction events that occurred in the gap between electrodes y_2 and y_3 of an orthogonal-strip detector. This data was acquired in the same manner as that of Figure 7. The absence of a significant dip in the distribution implies that charge is not collected at the gap surface between the two electrodes.

except this time the a-Ge layer was sputtered in an argon-hydrogen gas mixture. The addition of the hydrogen to the sputter gas caused more hydrogen to be incorporated into the deposited a-Ge film and resulted in a higher film resistivity. The resistance between the strips on this reprocessed detector was determined to be greater than 10^{14} Ω. With this detector, we repeated the measurements of Figure 7. The result shown in the intensity plot of Figure 11 indicates that the charge collection has been substantially improved. The large dip in the distribution of Figure 7 identifying the presence of a significant pulse-height deficit is not present in the plot of Figure 11. Furthermore, the events are more strongly distributed about the even-electrode pulse heights of zero and 59.5 keV in Figure 11 as compared to Figure 7. All of this suggests that the charge collection has gone from being predominantly of the type shown in Figure 6c to the desired types shown in Figures 6a and 6b. We also note that in these measurements when an event produced a pulse on only one of the readout channels (even-electrode pulse height of zero or 59.5 keV), the summed pulse height was this pulse height plus the noise floor of the other readout channel. Whereas when a pulse occurred on both readout channels, the noise floor was not included in the summed pulse height. This at least in part is the reason that the events with even-electrode pulse heights near zero and 59.5 keV have a slightly larger summed pulse height than the other events in the distribution.

The improved charge collection of this reprocessed detector then leads to better spectroscopic performance. Pulse-height spectra acquired with this detector are shown in Figures 9c and 10c. The ^{241}Am spectrum of Figure 9c has a reduced background and a slightly better energy resolution than that obtained when the detector had a lower resistivity contact layer (Figure 9a). The ^{137}Cs spectrum of Figure 10c further demonstrates the performance improvement as evidenced by the reduction in the low-energy background counts as compared to the Figure 10a spectrum. The good spectroscopic performance of this detector also indicates that the larger a-Ge film resistivity has not significantly inhibited the charge collection through the a-Ge layer to the electrode metallization. Based on this set of measurements and those made with other detectors, we conclude that the properties of the amorphous-semiconductor layer are critical when optimizing detectors for spectroscopic performance.

5. SUMMARY

The amorphous-semiconductor contact technology when applied to Ge-based detectors provides an effective means to produce the position-sensitive gamma-ray detectors necessary for applications requiring both imaging with good spatial resolution and high-resolution spectroscopy. We have produced a number of prototype orthogonal-strip detectors using this technology. With these detectors, it was demonstrated that the location of each gamma-ray interaction event in the detector could be determined in all three dimensions. In the directions parallel to the detector plane, the location is simply given by the positions of the strip electrodes that collect the electron and hole charge generated by the interaction event. In addition

to this standard detection in two dimensions, we were also able to extract the depth of the gamma-ray interaction event by measuring the time difference between the electron arrival at the anode strips and the hole arrival at the cathode strips. This three-dimensional determination of the gamma-ray interaction location should ultimately improve the image quality achieved with these detectors.

The spectroscopic performance of these detectors was also studied. Charge collection to the inter-electrode surface was observed in the detectors presumably because of the weak electric field region between adjacent strip electrodes. This incomplete charge collection can degrade energy resolution, reduce photopeak efficiency, and increase the number of background counts. Two approaches were successfully used to overcome this problem. In the first, field-shaping electrodes were placed between each charge-sensing electrode on the detector. With the appropriate application of bias between the field electrodes and the sensing electrodes, efficient charge collection to the sensing electrodes was produced. This then significantly improved the detector performance in terms of a reduced background and increased photopeak efficiency. The second approach consisted of increasing the resistivity of the amorphous-semiconductor layer. The basis for this was the idea that a high-resistivity surface layer at the gap between adjacent electrodes might accumulate enough charge to inhibit the further collection of charge to that surface. We demonstrated that a detector fabricated with a higher resistivity a-Ge contact film layer did indeed have more desirable charge collection properties and consequently achieved a better spectroscopic response.

ACKNOWLEDGMENTS

This research was supported in full under Contract No. DE-AC03-76SF00098, Environmental Management Science Program, Office of Science and Technology, Office of Environmental Management, United States Department of Energy (DOE). However, any opinions, findings, conclusions, or recommendations expressed herein are those of the authors' and do not necessarily reflect the views of DOE.

We thank M. T. Burks for helpful discussions during this work.

REFERENCES

1. R. P. Parker, E. M. Gunnersen, J. L. Wankling, and R. Ellis, "A semiconductor gamma camera with quantitative output," *Medical Radioisotope Scintigraphy*, pp. 71-85, International Atomic Energy Agency, Vienna, 1969.
2. J. F. Detko, "A prototype, ultra-pure germanium, orthogonal strip gamma-camera," *Medical Radioisotope Scintigraphy*, pp. 241-254, International Atomic Energy Agency, Vienna, 1973.
3. P. A. Schlosser, D. W. Miller, M. S. Gerber, R. F. Redmond, et al., "A practical gamma-ray camera system using high-purity germanium," *IEEE Trans. Nucl. Sci.* **21**, pp. 658-664, 1974.
4. L. Kaufman, V. Lorenz, K. Hosier, J. Hoenninger, et al., "Two-detector, 512-element high purity germanium camera prototype," *IEEE Trans. Nucl. Sci.* **25**, pp. 189-195, 1978.
5. D. Miller, P. Schlosser, A. Deutchman, J. Steidley, et al., "A multi-detector germanium gamma ray camera," *IEEE Trans. Nucl. Sci.* **26**, pp. 603-609, 1979.
6. P. N. Luke, "Gold-mask technique for fabricating segmented-electrode germanium detectors," *IEEE Trans. Nucl. Sci.* **31**, pp. 312-315, 1984.
7. D. Protic and G. Riepe, "Position-sensitive germanium detectors," *IEEE Trans. Nucl. Sci.* **32**, pp. 553-555, 1985.
8. D. Gutknecht, "Photomask technique for fabricating high purity germanium strip detectors," *Nucl. Instr. Meth. Phys. Res.* **A 288**, pp. 13-18, 1990.
9. A. Hamacher, H. Machner, M. Nolte, M. Palarczyk, et al., "Performance of position-sensitive germanium detectors in nuclear reaction experiments," *Nucl. Instr. Meth. Phys. Res.* **A 295**, pp. 128-132, 1990.
10. P. N. Luke, R. H. Pehl, and F. A. Dilmanian, "A 140-element Ge detector fabricated with amorphous Ge blocking contacts," *IEEE Trans. Nucl. Sci.* **41**, pp. 976-978, 1994.
11. P. N. Luke, M. Amman, B. F. Phlips, W. N. Johnson, et al., "Germanium orthogonal strip detectors with amorphous-semiconductor contacts," accepted for publication in *IEEE Trans. Nucl. Sci.*
12. W. L. Hansen and E. E. Haller, "Amorphous germanium as an electron or hole blocking contact on high-purity germanium detectors," *IEEE Trans. Nucl. Sci.* **24**, pp. 61-63, 1977.
13. P. N. Luke, C. P. Cork, N. W. Madden, C. S. Rossington, et al., "Amorphous Ge bipolar blocking contacts on Ge detectors," *IEEE Trans. Nucl. Sci.* **39**, pp. 590-594, 1992.
14. M. Amman and P. N. Luke, "Three-dimensional position sensing and field shaping in orthogonal-strip germanium gamma-ray detectors," *Nucl. Instr. Meth. Phys. Res.* **A**, accepted for publication.
15. M. Momayezi, W. K. Warburton, and R. Kroeger, "Position resolution in a Ge-strip detector," *SPIE* **3768**, pp. 530-537, 1999.

16. H. L. Malm, C. Canali, J. W. Mayer, M-A. Nicolet, et al., "Gamma-ray spectroscopy with single-carrier collection in high-resistivity semiconductors," *Appl. Phys. Lett.* **26**, pp. 344-346, 1975.
17. H. H. Barrett, J. D. Eskin, and H. B. Barber, "Charge transport in arrays of semiconductor gamma-ray detectors," *Phys. Rev. Lett.* **75**, pp. 156-159, 1995.
18. P. N. Luke, "Electrode configuration and energy resolution in gamma-ray detectors," *Nucl. Instr. Meth. Phys. Res.* **A 380**, pp. 232-237, 1996.
19. H. L. Malm and R. J. Dinger, "Charge collection in surface channels on high-purity Ge detectors," *IEEE Trans. Nucl. Sci.* **23**, pp. 76-80, 1976.
20. R. A. Street, *Hydrogenated Amorphous Silicon*, Cambridge University Press, New York, 1991, and references therein.
21. J. T. Walton, W. S. Hong, P. N. Luke, N. W. Wang, et al., "Amorphous silicon/crystalline silicon heterojunctions for nuclear radiation detector applications," *IEEE Trans. Nucl. Sci.* **44**, pp. 961-964, 1997.
22. R. S. Muller and T. I. Kamins, *Device Electronics for Integrated Circuits*, 2nd edition, p. 156, John Wiley & Sons, New York, 1986.
23. S. M. Sze, *Physics of Semiconductor Devices*, 2nd edition, p. 291, John Wiley & Sons, New York, 1981.
24. W. L. Hansen, E. E. Haller, and G. S. Hubbard, "Protective surface coatings on semiconductor nuclear radiation detectors," *IEEE Trans. Nucl. Sci.* **27**, pp. 247-251, 1980.
25. M. J. Berger and J. H. Hubbell, *XCOM: Photon Cross Sections Database*, National Institute of Standards and Technology, Gaithersburg, 1998.
26. G. Rossi, J. Morse, and D. Protic, "Energy and position resolution of germanium microstrip detectors at x-ray energies from 15 to 100 keV," *IEEE Trans. Nucl. Sci.* **46**, pp. 765-773, 1999.
27. R. A. Kroeger, N. Gehrels, W. N. Johnson, J. D. Kurfess, et al., "Charge spreading and position sensitivity in a segmented planar germanium detector," *Nucl. Instr. Meth. Phys. Res.* **A 422**, pp. 206-210, 1999.
28. W. Shockley, "Currents to conductors induced by a moving point charge," *J. Appl. Phys.* **9**, pp. 635-636, 1938.
29. S. Ramo, "Currents induced by electron motion," *Proc. I.R.E.* **27** pp. 584-585, 1939.